



Carboxymethyl- β -cyclodextrin conjugated magnetic nanoparticles as nano-adsorbents for removal of copper ions: Synthesis and adsorption studies

A.Z.M. Badruddoza, A.S.H. Tay, P.Y. Tan, K. Hidajat, M.S. Uddin*

Department of Chemical and Biomolecular Engineering, National University of Singapore, 10 Kent Ridge Crescent, Singapore 119260, Singapore

ARTICLE INFO

Article history:

Received 8 August 2010

Received in revised form 7 October 2010

Accepted 7 October 2010

Available online 15 October 2010

Keywords:

Magnetic nanoparticles

Carboxymethyl- β -cyclodextrin

Copper adsorption

Isotherms

Kinetic model

ABSTRACT

A novel nano-adsorbent, carboxymethyl- β -cyclodextrin modified Fe_3O_4 nanoparticles (CMCD-MNPs) is fabricated for removal of copper ions from aqueous solution by grafting CM- β -CD onto the magnetite surface via carbodiimide method. The characteristics results of FTIR, TEM, TGA and XPS show that CM- β -CD is grafted onto Fe_3O_4 nanoparticles. The grafted CM- β -CD on the Fe_3O_4 nanoparticles contributes to an enhancement of the adsorption capacity because of the strong abilities of the multiple hydroxyl and carboxyl groups in CM- β -CD to adsorb metal ions. The adsorption of Cu^{2+} onto CMCD-MNPs is found to be dependent on pH and temperature. Adsorption equilibrium is achieved in 30 min and the adsorption kinetics of Cu^{2+} is found to follow a pseudo-second-order kinetic model. Equilibrium data for Cu^{2+} adsorption are fitted well by Langmuir isotherm model. The maximum adsorption capacity for Cu^{2+} ions is estimated to be 47.2 mg/g at 25 °C. Furthermore, thermodynamic parameters reveal the feasibility, spontaneity and exothermic nature of the adsorption process. FTIR and XPS reveal that Cu^{2+} adsorption onto CMCD-MNPs mainly involves the oxygen atoms in CM- β -CD to form surface-complexes. In addition, the copper ions can be desorbed from CMCD-MNPs by citric acid solution with 96.2% desorption efficiency and the CMCD-MNPs exhibit good recyclability.

© 2010 Elsevier B.V. All rights reserved.

1. Introduction

Heavy metal pollution in industrial wastewater has attracted global attention because of its adverse effects on the environment and human health [1,2]. It is, therefore, crucial to remove these heavy metals from wastewaters effectively before their discharge into the environment. Currently heavy metal removal methods include chemical precipitation, ion exchange, liquid–liquid extraction, membrane filtration, adsorption and biosorption [3]. Among these methods, adsorption has increasingly received more attention as it is simple and cost effective [4,5].

Recently, adsorption using magnetic nano-sized adsorbents has attracted significant attentions due to the specific characteristics [2,5–9]. Their basic properties, extremely small size, high surface-area-to volume ratio and the absence of internal diffusion resistance provides better kinetics for adsorption of metal ions from aqueous solution. Magnetic nano-adsorbents have the advantages of both magnetic separation techniques and nano-sized materials, which can be easily recovered or manipulated with an external magnetic field. Moreover, the incorporation of magnetic particles with other functionalized materials such as multi-walled carbon nanotubes (MWCNT) [10–12], zeolites [13], activated car-

bon [14] etc., which are effective for the removal of both organic and inorganic pollutants is potentially a promising method to facilitate the separation and recovery of the adsorbents. Various types of magnetic nano-adsorbents with tailored surface reactivity by using natural or synthetic polymers such as, chitosan, gum arabic, alginate, poly(acrylic acid) etc., have been used recently for heavy metal removal from wastewater [2,5–8,10,15–17]. However, the effectiveness of magnetic nano-adsorbents modified with cyclodextrin – an important class of polysaccharides has not been discussed yet.

β -cyclodextrin (β -CD) is a cyclic oligosaccharide consist of seven α -D-glucose units connected through α -(1,4) linkages. The structure of these molecules is toroidal, truncated cones containing an apolar cavity with primary hydroxyl groups lying on the outside and the secondary hydroxyl groups inside [18,19]. Cyclodextrins can form inclusion complexes with a wide variety of organic and inorganic compounds in its hydrophobic cavity [18]. Although there is less report on environmental applications of cyclodextrins for heavy metal removal, there is evidence that metal can be complexed by cyclodextrins through hydroxyl groups. Metal ion complexes with cyclodextrins could have a wide range of applications in catalysis and molecular recognition [20]. Some properties such as aqueous solubility and metal complexation potential can be altered by substituting functional groups to the outside of the cyclodextrin [21]. For example, carboxymethyl- β -cyclodextrin (CM- β -CD) has the ability to complex heavy metals such as cadmium, nickel, strontium and mercury through the interactions

* Corresponding author. Tel.: +65 6516 2886; fax: +65 6779 1936.

E-mail address: cheshabb@nus.edu.sg (M.S. Uddin).

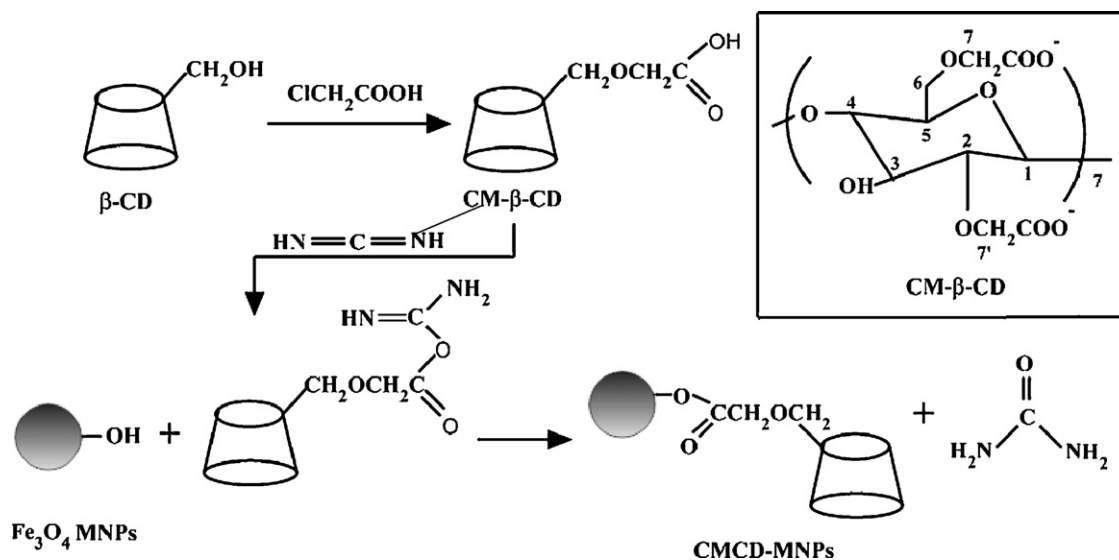


Fig. 1. An illustration for the carboxymethylation and binding of cyclodextrin onto Fe_3O_4 nanoparticles.

between the metal ions and $-\text{COOH}$ functional groups [22,23]. Insoluble cyclodextrin polymers and cyclodextrin immobilized on various supports including inorganic carriers are currently being investigated for adsorptive specificity towards heavy metal ions [24,25]. Very recently, Hu et al. showed that the grafted β -CD on the MWCNT/iron oxides contributes to an enhancement of the adsorption capacity because of the strong complexation abilities of the multiple hydroxyl groups in β -CD with the lead ions [12]. However, to our knowledge, no adsorptive study of heavy metals on magnetic nanoparticles covalently bonded with $\text{CM-}\beta\text{-CD}$ has been reported so far. The high surface area to volume ratio of the Fe_3O_4 nanoparticles and magnetic properties together with the adsorption capabilities of $\text{CM-}\beta\text{-CD}$ through complex formation would facilitate the removal of heavy metals from wastewater.

In this study, a novel magnetic nano-adsorbent was synthesized for the adsorption of metal ions by surface modification of Fe_3O_4 nanoparticles with $\text{CM-}\beta\text{-CD}$. The adsorption behavior of these sorbents was investigated using Cu^{2+} as the target metal contaminant because of its extensive environmental impacts. The effects of several factors such as, pH, initial Cu^{2+} concentration and temperature were also studied. The adsorption mechanisms of Cu^{2+} onto CMCD-MNPs were investigated through FTIR and XPS analyses. In addition, the regeneration and reusability of the adsorbents were also evaluated.

2. Experimental details

2.1. Materials

In this work, the following chemicals were used for fabricating CMCD-MNPs : iron (II) chloride tetrahydrate (99%) [Alfa Aesar], iron (III) chloride hexahydrate (98%) [Alfa Aesar], ammonium hydroxide (25%) [Merck], β -cyclodextrin (β -CD, 99%) [Tokyo Kasei Kogyo (Japan)], carbodiimide (cyanamide, CH_2N_2 , 98%) [Sigma], copper (II) nitrate [Sigma], chloroacetic acid (99%) [Alfa Aesar]. All other chemicals were of analytical grade and used as received without further purification.

2.2. Methods

2.2.1. Preparation of carboxymethyl- β -cyclodextrin ($\text{CM-}\beta\text{-CD}$)

$\text{CM-}\beta\text{-CD}$ was prepared following the procedure of literature [26], and the detail synthesis of $\text{CM-}\beta\text{-CD}$ was as following: a mix-

ture of β -CD (10 g) and NaOH (9.3 g) in water (37 mL) was treated with a 16.3% monochloroacetic acid solution (27 mL) at 50°C for 5 h. Then the reaction mixture was cooled to room temperature, and pH was adjusted (6–7) using HCl. The obtained neutral solution was then poured to superfluous methanol solvent and white precipitates were produced. The solid precipitation was then filtered and dried under vacuum to give carboxymethylated β -CD ($\text{CM-}\beta\text{-CD}$, 6 g). $^1\text{H NMR}$ (300 MHz, D_2O), δ (TMS, ppm): 5.08, 5.30 (s, 7H, H-1), 4.39 (s, 2.5H, H-7), 3.30–4.20 (m, 45.7H, H-2, H-3, H-4, H-5, H-6, H-7'). (The number of C is shown in Fig. 1.) IR (KBr): ν (cm^{-1}): 3140–3680 ($-\text{OH}$), 2923 ($-\text{CH}$), 1741 ($\text{C}=\text{O}$), 960–1200 ($\text{C}-\text{O}-\text{C}$, $\text{C}-\text{C}/\text{C}-\text{O}$) (Fig. 2c).

2.2.2. Fabrication of $\text{CM-}\beta\text{-CD}$ modified Fe_3O_4 nanoparticles (CMCD-MNPs)

Firstly, magnetite nanoparticles were prepared by chemical coprecipitation method as described in previous work [27,28]. In brief, a complete precipitation of Fe_3O_4 was achieved under alkaline condition, while maintaining a molar ratio of $\text{Fe}^{2+}:\text{Fe}^{3+} = 1:2$ under an inert environment. The binding of $\text{CM-}\beta\text{-CD}$ onto the Fe_3O_4 surface was conducted following our previous work [28]. For the grafting of $\text{CM-}\beta\text{-CD}$, 100 mg of magnetic nanoparticles were first added to 2 mL of buffer A (0.003 M phosphate, pH 6, 0.1 M NaCl) and sonicated for 10 min. Then, the reaction mixture was

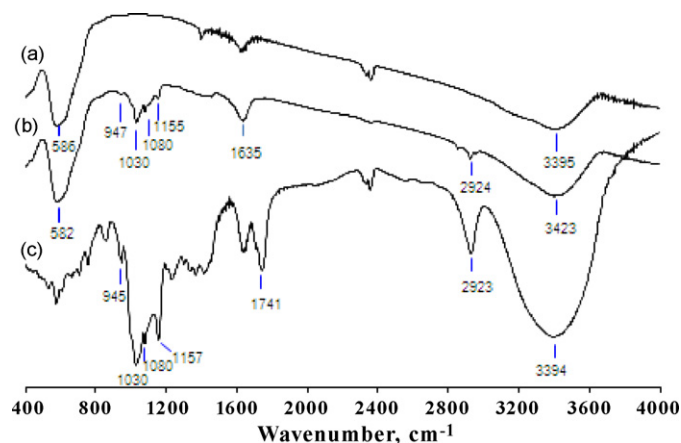


Fig. 2. FTIR spectra of (a) uncoated Fe_3O_4 MNPs, (b) CMCD-MNPs , and (c) $\text{CM-}\beta\text{-CD}$.

further sonicated for 15 min after adding 0.5 mL of carbodiimide solution (0.025 g mL^{-1} in buffer A). Finally, 2.5 mL of CM- β -CD (10–120 mg/mL in buffer A) was added and the reaction mixture was sonicated for another 90 min. The resulting nanoparticles were recovered from the reaction mixture using a permanent magnet and washed 2–3 times with buffer A and then dried in a vacuum oven.

2.2.3. Characterizations of magnetic nanoparticles

A bright-field TEM (Model-JEM 2010) was used to determine the size and morphology of magnetic nanoparticles. Fourier transform infrared (FTIR) spectroscopy measurements were performed by Bio-Rad model 400 using KBr as background over the range of $4000\text{--}400 \text{ cm}^{-1}$. X-ray photoelectron spectroscopy (XPS) analysis was carried out on a VG ESCALAB MkII spectrometer with a MgK α X-ray source (1253.5 eV photons) to determine the elements such as C, O and Cu atoms present. All binding energies were referenced to the neutral C 1s peak at 284.6 eV. The thermogravimetric analysis (TGA) was performed on a thermal analysis system (Model: TA 2050). For TGA measurements, the weight loss of dried sample was monitored under N_2 from room temperature to 800°C at a rate of $10^\circ\text{C}/\text{min}$. The zeta potentials of as-synthesized nanoparticles were measured at different pH using a Malvern ZEN2600 Zetasizer Nano ZS.

2.2.4. Adsorption and desorption studies

The adsorption of Cu^{2+} by the CMCD-MNPs (as a magnetic nano-adsorbent) was investigated using batch equilibrium technique in aqueous solutions at pH 2–6 at $25\text{--}55^\circ\text{C}$. In general, 120 mg of wet magnetic nano-adsorbent was added to 10 mL of copper nitrate solution of various concentrations and shaken in a thermostatic water-bath shaker operated at 230 rpm. After equilibrium was reached, the magnetic nano-adsorbents were removed using a strong permanent magnet made of Nd-Fe-B and the supernatant was collected. The solution pH was adjusted by NaOH or HCl. The concentrations of copper ions were measured using atomic absorption spectrometer (Agilent ICP-MS 7700 series).

For the kinetic experiments, the initial copper ion concentrations were 50, 100 and 200 mg/L and the initial solution pH value was 6.0 (the solution pH was not controlled during the experiments). These copper solutions containing the magnetic particles were agitated for a contact time varied in the range of 0–240 min at a speed of 230 rpm at 25°C . At various time intervals, samples were collected after separation of magnetic adsorbents by magnetic decantation process and the copper concentration was determined as mentioned previously. In the investigation of the effect of solution pH on equilibrium copper adsorption, the initial Cu^{2+} concentrations in the solution were 50 and 200 mg/L, but the solution pH values were changed from 2 to 6. In the adsorption isotherm experiments, the initial solution pH was 6.0 while the initial Cu^{2+} concentrations in the solutions were changed from 50 to 400 mg/L and temperatures were varied from 25°C to 55°C . The samples were shaken for 4 h (which was enough to achieve equilibrium) at 230 rpm. Duplicate experiments were carried out in each case and the reproducibility was found to be fairly good. The error percentage was within 5%.

Desorption study was conducted using 0.1 M acetic acid, 0.1 M citric acid and 0.1 M Na_2EDTA as desorption eluents. Adsorption was first conducted using 120 mg of wet CMCD-MNPs in 10 mL of 200 mg/L Cu^{2+} solution for 4 h at pH 6. Desorption was then studied by adding 10 mL of either acid solution to the Cu^{2+} -sorbed CMCD-MNPs. After shaking at 200 rpm for 3 h, the CMCD-MNPs were removed and the concentration of copper ions was measured.

3. Results and discussions

3.1. Synthesis and characterization of magnetic nanoparticles

CMCD-MNPs (BET surface area $\sim 110.9 \text{ m}^2/\text{g}$) were synthesized using a two-steps procedure. The first step involves the formation of carboxyl group onto β -CD by reacting chloroacetic acid with β -CD in the alkaline condition. The average number of carboxylate groups (3.1) per molecule of CM- β -CD is determined using $^1\text{H NMR}$ [29] as well as by titrating the carboxylate groups with NaOH solution [21]. Before titrating CM- β -CD with NaOH, the CM- β -CD -Na salt was converted to its acidic form by passing 50 ml of a 100 g/L CM- β -CD solution twice through a column containing an ion exchange resin (H^+). Using the degree of substitution of 3.1 carboxymethyl substituents (each with a molecular weight of 58 amu) per CM- β -CD molecule, we calculated an average atomic mass for CM- β -CD of 1312 amu. This molecular weight was used to calculate the grafted amount of CM- β -CD on the surface of Fe_3O_4 nanoparticles. In the second step, CM- β -CD was covalently bonded onto the surface of magnetic nanoparticles via carbodiimide activation as shown in Fig. 1. Here, the $-\text{COOH}$ functional groups on CM- β -CD reacted with surface $-\text{OH}$ groups to form metal carboxylate (COOM).

The grafting of CM- β -CD on surfaces of magnetic nanoparticles is confirmed by FTIR spectroscopy. Fig. 2 shows the FTIR spectra of uncoated MNPs, CMCD-MNPs and CM- β -CD in the $400\text{--}4000 \text{ cm}^{-1}$ wave number range. It is shown that the characteristic adsorption band of Fe-O bonds in the tetrahedral sites is 586 cm^{-1} which is shifted to 582 cm^{-1} after surface modification with CM- β -CD. The broad band at $3300\text{--}3500 \text{ cm}^{-1}$ is due to $-\text{OH}$ stretching vibrations. The peak at 1741 cm^{-1} in CM- β -CD spectrum is assigned to C=O stretching vibration of carbonyl groups which indicates the attachment of carboxymethyl group on β -CD. The spectrum of CMCD-MNPs shows the characteristic peaks at 945, 1030, 1157 and 1635 cm^{-1} . The peak at 945 cm^{-1} is due to the R-1,4-bond skeleton vibration of β -CD, and the peaks at 1030 and 1157 cm^{-1} corresponds to the antisymmetric glycosidic ν_a (C-O-C) vibrations and coupled ν (C-C/C-O) stretch vibration [30]. The peak at 1635 cm^{-1} is assigned C=O stretching of carboxylate [31]. The absorption band at 2924 cm^{-1} corresponds to asymmetric C-H stretching vibration. All the significant peaks of CM- β -CD in the range of $900\text{--}1200 \text{ cm}^{-1}$ are present in the spectrum of CMCD-MNPs with a small shift. Thus, it can be concluded that CM- β -CD has been grafted successfully on the surface of Fe_3O_4 nanoparticles.

Typical TEM image and size distribution of CMCD-MNPs are shown in Fig. 3. Well-shaped spherical or ellipsoidal magnetic nanoparticles are observed. The mean diameter of CM- β -CD coated magnetic nanoparticles is about 12 nm which is slightly higher than that of uncoated magnetic nanoparticles (mean diameter $\sim 11.0 \text{ nm}$). This indicates that the binding process did not result in agglomeration and the change in the size of the nanoparticles. No detectable layer due to CM- β -CD can be observed on magnetic nanoparticles.

The amount of CM- β -CD grafted on Fe_3O_4 MNPs is estimated from TGA analyses of uncoated and CM- β -CD coated magnetic nanoparticles. As shown in Fig. 4(a), the TGA curve of uncoated MNPs shows first weight loss of 1.6% below 130°C which might be due to the loss of adsorbed water in the sample. After this brief event of weight loss, an unexpected weight gain takes place within the temperature range from 130 to 205°C . This weight gain can be attributed to the oxidation of Fe_3O_4 to Fe_2O_3 [32]. However, a dominant phase of Fe_3O_4 is formed which is evidenced by XRD results (figure not shown). The total weight loss over the full temperature range is estimated to be 2.3% due to the loss of the adsorbed water as well as dehydration of the surface $-\text{OH}$ groups. The TGA curve for CMCD-MNPs exhibits two steps of weight loss, contributed from the loss of residual water in the sample in $30\text{--}190^\circ\text{C}$ and the loss

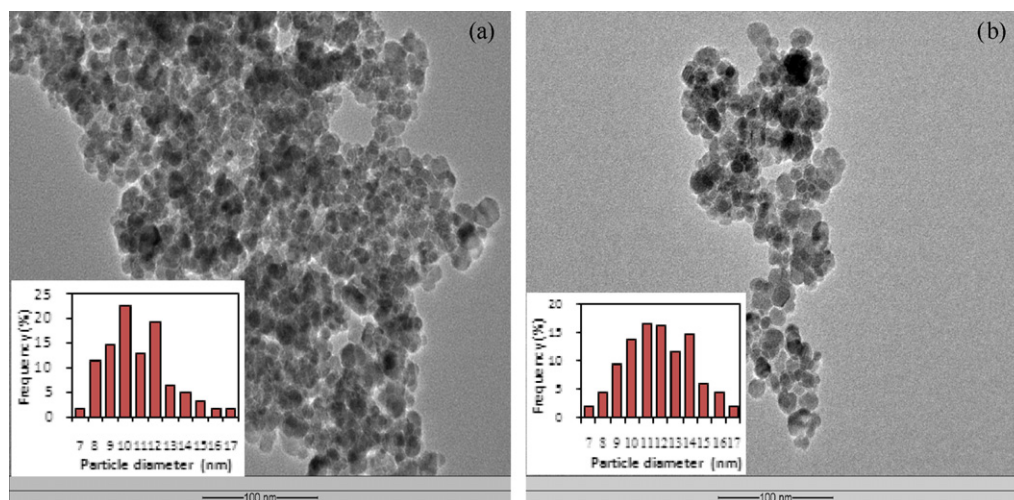


Fig. 3. TEM micrographs and size distributions of (a) uncoated and (b) CM- β -CD bound Fe_3O_4 magnetic nanoparticles. (Scale bar is 100 nm).

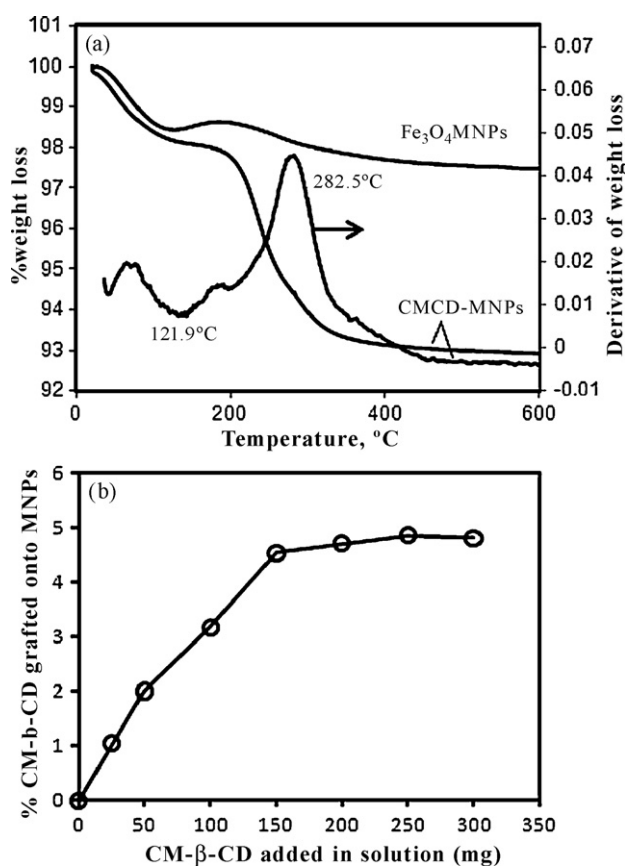


Fig. 4. (a) TGA curves for uncoated Fe_3O_4 MNPs and CMCD-MNPs; (b) effect of the amount of CM- β -CD in solution on the grafted CM- β -CD contents onto magnetic nanoparticles.

of CM- β -CD in the range of 200–450 °C. A drastic drop of weight loss can be seen in the range of 190–400 °C with the occurrence of a weak heat absorption at 282.5 °C and it is contributed from the thermal decomposition of CM- β -CD. Thus, the TGA curves also confirm the successful grafting of CM- β -CD onto the magnetic surface.

The effect of the amount of CM- β -CD used in solution on the amount of grafted CM- β -CD onto the surface of magnetic nanoparticles was also demonstrated in this study. The experiment was performed in 5 mL of CM- β -CD (5–60 mg/mL) solution containing a constant amount of Fe_3O_4 (100 mg). The percentage amount of CM-

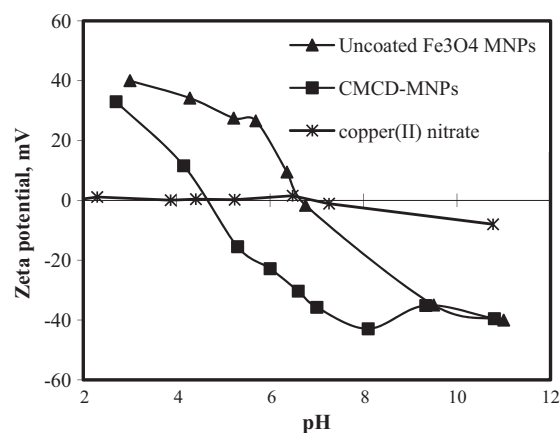


Fig. 5. Zeta potentials of uncoated and CM- β -CD coated magnetic nanoparticles at different pH.

β -CD grafted on Fe_3O_4 MNPs was estimated from the weight loss measured by TGA analysis. As shown in Fig. 4(b), with increasing amounts of CM- β -CD in solution, the amount of grafted CM- β -CD on the nanoparticles increases first and then remains almost constant when the amount of CM- β -CD in solution is above 150 mg. This may be due to the fact that as the amount of Fe_3O_4 is fixed which means the number of surface hydroxyl ($-\text{OH}$) groups are fixed, no more $-\text{OH}$ groups are available which can react with the $-\text{COOH}$ groups on CM- β -CD to form metal carboxylate. Similar findings were reported in covalent binding of poly(acrylic acid) (PAA) to Fe_3O_4 nanoparticles via carbodiimide activation [33]. However, the maximum amount of CM- β -CD bound to Fe_3O_4 nanoparticles could be determined to be 4.8 wt%, i.e., 0.0366 mmol/g.

Zeta potentials of uncoated and CM- β -CD coated magnetic nanoparticles (0.1 mg/ml) were measured in 10^{-3} M NaCl aqueous solution at different pH. The solution pH was adjusted by NaOH or HCl. As shown in Fig. 5, the pH value of point of zero charge (pH_{pzc}) of uncoated Fe_3O_4 nanoparticles is about 6.8, consistent with the values reported in literature. After being grafted with CM- β -CD, the pH_{pzc} has been shifted to 4.7, indicating that the grafting of CM- β -CD onto uncoated MNPs is successful. Moreover, magnetic nanoparticles modified with CM- β -CD yields acidic surface since pH_{pzc} is lower than that of uncoated MNPs and this surface acidity is due to the introduction of several oxygen-containing functional groups [34].

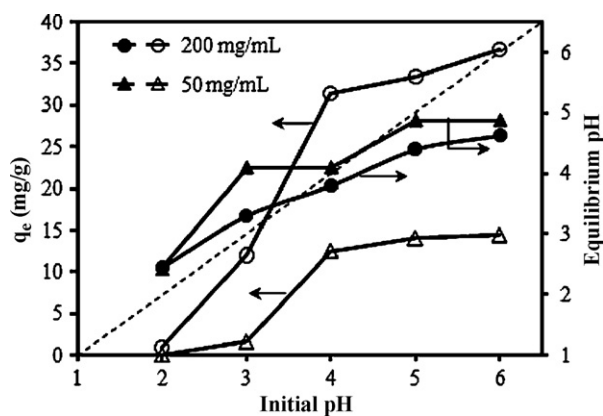


Fig. 6. Effect of pH on the adsorption of Cu^{2+} ions by CMCD-MNPs at 25 °C. Open points: q_e versus initial pH values; solid points: equilibrium pH values versus initial pH values.

3.2. Adsorption of Cu^{2+} ions onto CMCD-MNPs

3.2.1. Effect of initial pH

The pH of the aqueous solution is an important controlling parameter in the adsorption process [2,4,35]. The effects of initial solution pH on Cu^{2+} adsorption onto CMCD-MNPs were investigated at pH 2–6, 25 °C, and an initial Cu^{2+} ion concentration of 50 and 200 mg/L. As shown in Fig. 6, it is noteworthy that the adsorption capacity of Cu^{2+} ions increases with the solution pH at an initial Cu^{2+} concentration of 200 mg/L. This might be due to the less insignificant competitive adsorption of hydrogen ions [7,8,36]. At a lower initial Cu^{2+} concentration (50 mg/L), the adsorption capacity increases with increasing the solution pH and then remains almost unchanged at pH 4–6. This might be due to the fact that almost all Cu^{2+} ions are adsorbed. It is well known that Cu(II) species can be present in aqueous solution in the forms of Cu^{2+} , $\text{Cu}(\text{OH})^+$, $\text{Cu}(\text{OH})_2$, $\text{Cu}(\text{OH})_3^-$ and $\text{Cu}(\text{OH})_4^{2-}$ and the predominant copper species at pH < 6.0 is Cu^{2+} [35,37]. Therefore, less adsorption of Cu^{2+} that takes place on CMCD-MNPs at lower pH, can be explained by the fact that at these pH values the H^+ concentration is high, which can compete with copper cations for the same adsorption sites [35]. The adsorption studies at pH > 6 were not conducted because of the precipitation of $\text{Cu}(\text{OH})_2$ from the solution.

The effect of pH can be also explained by considering the surface charge on the adsorbent material. We attempted to find the zeta potential of Cu^{2+} solution and Fig. 5 shows that copper solution has positive zeta potential at pH < 7. Since the zeta potentials of the CMCD-MNPs are positive at pH < 4.7 (point of zero charge, pH_{pzc}), the interactions between the adsorption sites on CMCD-MNPs and the copper ions are electrostatically repulsive. As the solution pH increases, the repulsion between adsorbent surface and metal ions becomes weaker, thus enhancing the adsorption capacity [38]. On contrary, at pH above pH_{pzc} , the negatively charged CMCD-MNPs nano-adsorbents attract the positively charged metal ions. Moreover, the adsorption of Cu^{2+} ions depends on the adsorption sites available for copper attachment on the surface of CMCD-MNPs, possibly through the complexation with mainly $-\text{OH}$ and $-\text{COOH}$ functional groups (see the discussions in the Section 3.2.5). The equilibrium pH values are also plotted as a function of initial pH values for each experimental data (Fig. 6). One can see that the final pH value is higher than the initial pH value for lower pH range. For initial solution pH values above 4.0, the final pH value is lower than the initial one and this difference becomes higher for higher adsorption capacity of CMCD-MNPs. The pH decreasing after Cu^{2+} adsorption suggests that part of H^+ is released from the CMCD-MNPs surface to solution. Due to the increase of pH, more surface

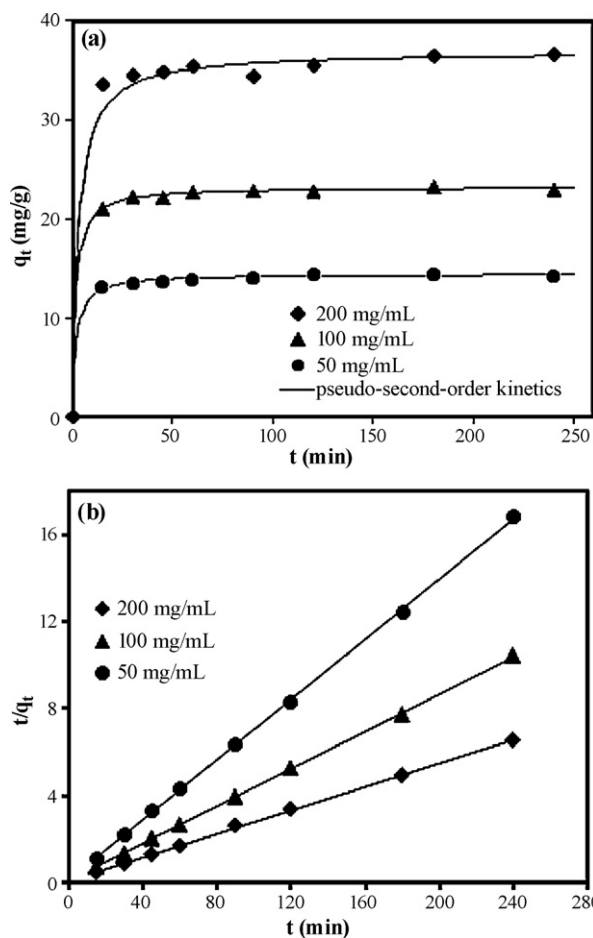


Fig. 7. (a) Effect of contact time on Cu^{2+} adsorption by CMCD-MNPs; (b) pseudo-second-order kinetics for adsorption of Cu^{2+} (Initial pH 6, temperature: 25 °C).

functional groups are deprotonated to provide more metal binding sites, which results in a high metal ion adsorption and more H^+ are released into the solution resulting in the decrease in the pH values after metal adsorption [35].

3.2.2. Adsorption kinetics

Fig. 7a shows the effects of contact time on adsorption of Cu^{2+} onto CMCD-MNPs at different Cu^{2+} concentrations ranging from 50 to 200 mg/mL and at 25 °C. It can be seen that a rapid adsorption of Cu^{2+} by CMCD-MNPs occurs, with equilibrium reached in approximately 30 min. The adsorption capacity increases as initial metal ion concentration increases. Within 15 min, 90% of Cu^{2+} adsorption equilibrium is achieved using CMCD-MNPs. This suggests that CMCD-MNPs could easily and rapidly adsorb Cu^{2+} from aqueous solution due to high specific surface area and the absence of internal diffusion resistance. Rapid adsorption rate for copper removal has also been observed using several magnetic nanoparticles based nano-adsorbents [5,7,16]. However, a shaking time of 4 h was used in all further adsorption experiments to ensure equilibrium.

The adsorption kinetics of Cu^{2+} onto CMCD-MNPs is investigated with the help of two kinetic models, namely the Lagergren pseudo-first-order and pseudo-second-order model. The pseudo-first-order kinetic model is expressed by the following equation [39]:

$$\ln(q_e - q_t) = \ln q_e - k_1 t \quad (1)$$

where q_e and q_t refer to the adsorption capacity of Cu^{2+} (mg/g) at equilibrium and at any time, t (min), respectively, and k_1 is the rate constant of pseudo-first-order adsorption (min^{-1}). The slope of the

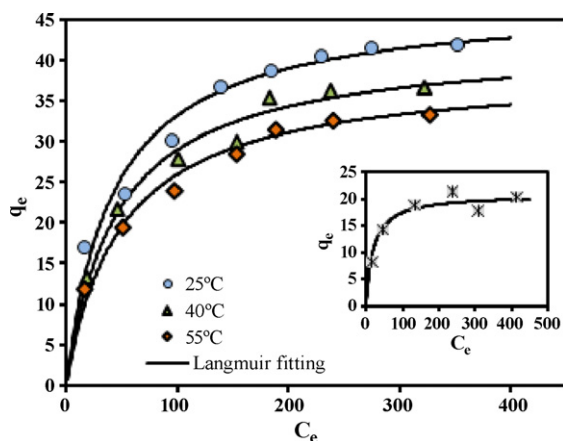


Fig. 8. Equilibrium isotherms for Cu^{2+} adsorption by CMCD-MNPs at different temperature and by uncoated Fe_3O_4 nanoparticles (inset) at 25°C and initial pH 6.

linear plot of $\log(q_e - q_t)$ versus t is used to determine k_1 (figure not shown).

The pseudo-second-order kinetic rate equation is expressed as follows [40]:

$$\frac{t}{q_t} = \frac{1}{k_2 q_e^2} + \frac{1}{q_e} t \quad (2)$$

where k_2 is the rate constant of pseudo-second-order adsorption ($\text{g mg}^{-1} \text{min}^{-1}$). The slope and intercept of the plot of t/q_t versus t are used to calculate k_2 and $q_{e,\text{cal}}$ (Fig. 7b). The corresponding kinetic parameters from both models are listed in Table 1. It is found that the correlation coefficients (R^2) for the pseudo-first-order kinetic model are less than 90% indicating a poor pseudo-first-order fit to the experimental data. On the other hand, the correlation coefficient (R^2) for the pseudo-second-order adsorption model has high value (>99%), and the q_e values ($q_{e,\text{cal}}$) calculated from pseudo-second-order model are more consistent with the experimental q_e values ($q_{e,\text{exp}}$) than those calculated from pseudo-first-order model. These facts suggest that the adsorption data are well represented by pseudo-second-order kinetic model. The pseudo-second-order adsorption has also been reported for many adsorbents such as natural kaolinite clay [41], H_2SO_4 modified chitosan [42], chitosan-coated MNPs modified with alpha-ketoglutaric acid [17].

3.2.3. Adsorption isotherm of Cu^{2+} ions

The equilibrium isotherms for the adsorption of copper ions by uncoated MNPs at 25°C and by CMCD-MNPs at different temperatures (25°C , 40°C and 55°C) in pH 6 are shown in Fig. 8. The equilibrium data are fitted by Langmuir and Freundlich isotherm equations [43]. The Langmuir equation can be expressed as:

$$\frac{C_e}{q_e} = \frac{C_e}{q_m} + \frac{1}{q_m K_L} \quad (3)$$

where q_e is the amount of adsorbed material at equilibrium (mg/g), C_e the equilibrium concentration in solution (mg/L), q_m the maximum capacity of adsorbent (mg/g), and K_L is the "affinity parameter" or Langmuir constant (L/mg). The linear form of Freundlich equation, which is an empirical equation derived to model

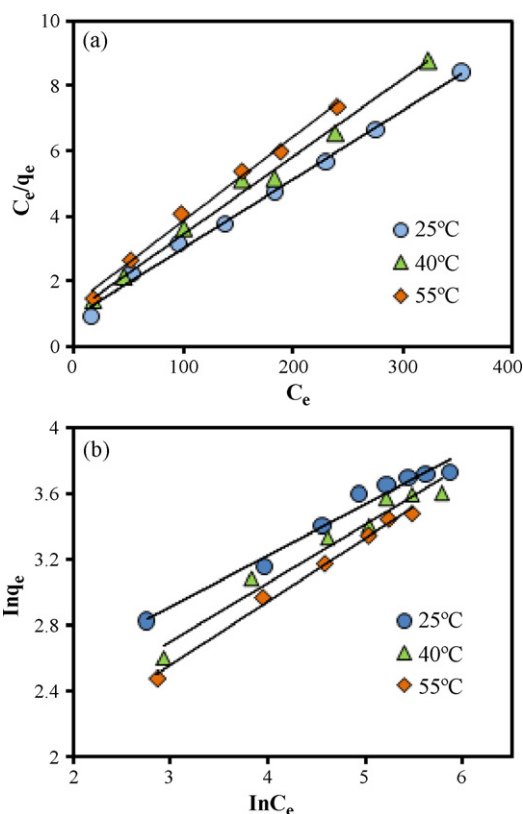


Fig. 9. The Langmuir (a) and Freundlich (b) isotherm plots for Cu^{2+} adsorption by CMCD-MNPs at pH 6.

the multilayer adsorption, can be represented as follows:

$$\ln q_e = \frac{1}{n} \ln C_e + \ln K_F \quad (4)$$

where q_e and C_e are defined as above, K_F is Freundlich constant (L/mg), and n is the heterogeneity factor.

The values of q_m and K_L are determined from the slope and intercept of the linear plots of C_e/q_e versus C_e (Fig. 9a) and the values of K_F and $1/n$ are determined from the slope and intercept of the linear plot of $\ln q_e$ versus $\ln C_e$ (Fig. 9b). The isotherm parameters are shown in Table 2. Namely, in all temperature studied, the Langmuir isotherm shows a better fit to experimental data in compared to the Freundlich isotherm. Moreover, Table 2 shows that the Langmuir constant, K_L , related to the affinity of binding sites decreases with increasing temperature indicating that the adsorption is favorable at lower temperatures. The maximum adsorption capacities (q_m) (Table 2) for uncoated MNPs and CMCD-MNPs are found to be 20.8 and 47.2 mg/g, respectively, at 25°C . The q_m for uncoated MNPs is found quite similar as done by Banerjee and Chen (19.3 mg/g) [5]. CMCD-MNPs, on the other hand, could adsorb copper ions almost or more than twice that by uncoated MNPs indicating that the modification of magnetite surface by CM- β -CD which has multiple hydroxyl and carboxyl functional groups could enhance the adsorption capabilities. Hu et al. [12] also found that introducing cyclodextrin onto the surface of MWCNT/iron oxide

Table 1
Adsorption kinetic parameters of Cu^{2+} onto CMCD-MNPs.

Initial conc. C_0 (mg/mL)	Pseudo-first-order			Pseudo-second-order			
	k_1 (min^{-1})	$q_{e,\text{cal}}$ (mg/g)	R^2	$q_{e,\text{exp}}$ (mg/g)	k_2 , g/(mg min)	$q_{e,\text{cal}}$ (mg/g)	R^2
50	0.0053	10.92	0.688	14.88	0.038	14.47	0.999
100	0.0082	20.45	0.641	23.48	0.027	23.25	0.999
200	0.0116	34.75	0.896	36.77	0.009	36.90	0.999

Table 2Adsorption isotherm parameters for Cu²⁺ adsorption on uncoated and CM-β-CD coated magnetic nanoparticles at pH 6.

Adsorbents	T (°C)	Langmuir isotherm constants			Freundlich isotherm constants		
		K _L (L/mg)	q _m (mg/g)	R ²	K _F (mg/g)(L/mg)	n	R ²
CMCD-MNPs	25	0.0237	47.20	0.995	7.064	3.15	0.973
	40	0.0221	42.01	0.993	5.044	2.78	0.961
	55	0.0202	38.75	0.992	4.002	2.57	0.993
Uncoated MNPs	25	0.0514	20.80	0.984	4.635	3.86	0.853

Table 3Comparison of maximum adsorption capacity of CMCD-MNPs with those of some other magnetic adsorbents reported in literature for Cu²⁺ adsorption.

Adsorbents	Maximum adsorbed amount, q _m (mg/g)	References
Chitosan-coated MNPs modified with alpha-ketoglutaric acid	96.15	[2]
Glutaraldehyde modified MNPs (GA-APTES-NPs)	61.07	[16]
Calcium alginate modified MNPs	60.00	[6]
CM-β-CD modified MNPs	47.20	This study
Gum Arabic modified MNPs	38.50	[5]
Amino functionalized Fe ₃ O ₄ @ SiO ₂ core-shell NPs	29.85	[45]
Chitosan bound MNPs	21.50	[7]
Uncoated Fe ₃ O ₄ nanoparticles	19.30	[5]
Amino-functionalized MNPs	12.43	[8]
Carbon encapsulated MNPs	3.21	[46]

composites enhanced the adsorption capacity with Pb(II). Chen et al. [10] studied the adsorption of Eu(III) onto CNT-iron oxide composite in presence of poly(acrylic acid) (PAA) as a surrogate for natural organic matter and found that the presence of PAA could strongly enhance the Eu(III) adsorption and adsorbed PAA anions can be considered as a 'bridge' between the magnetic composite and Eu(III). A positive effect of PAA on Ni²⁺ adsorption at pH < 8 using MWCNT was also reported by Yang et al. [44]. The high complexation ability of pre-adsorbed PAA onto oxidized MWCNT with Ni²⁺ contributes to enhanced adsorption on the surfaces. The maximum uptake of Cu²⁺ by CMCD-MNPs obtained in this work is compared with other results reported in literature shown in Table 3. However, the adsorption capacity of CMCD-MNPs for copper ions is comparatively higher than some of other magnetic particles based adsorbents.

3.2.4. Effect of temperature and thermodynamic parameters

The effect of temperature on the adsorption isotherm was investigated under isothermal conditions in the temperature range of 25–55 °C and at pH 6. As shown in Fig. 8, the adsorption capacities for CMCD-MNPs decrease with the increase in temperature from 25 °C to 55 °C. Thermodynamic parameters such as change in free energy (ΔG°), enthalpy (ΔH°), and entropy (ΔS°) are calculated using the following thermodynamic functions:

$$\Delta G^\circ = -RT \ln K_p \quad (5)$$

$$\ln K_p = -\frac{\Delta H^\circ}{RT} + \frac{\Delta S^\circ}{R} \quad (6)$$

K_p is the thermodynamic equilibrium constant, i.e., the ratio of the equilibrium concentration of Cu²⁺ on CMCD-MNPs to that in solution. This constant K_p for the sorption process is determined by plotting ln(q_e/C_e) versus q_e and extrapolating to zero q_e [47,48]. Fig. 10 shows the van't Hoff plots of ln K_p versus 1/T (R² = 0.99) and the values of ΔH° and ΔS° for CMCD-MNPs are determined from the slopes and intercepts, respectively. The calculated thermodynamic parameters are listed in Table 4. The negative value of all ΔG° indicates the feasibility of the process and spontaneous nature

Table 4Thermodynamic parameters for the adsorption of Cu²⁺ onto CMCD-MNPs.

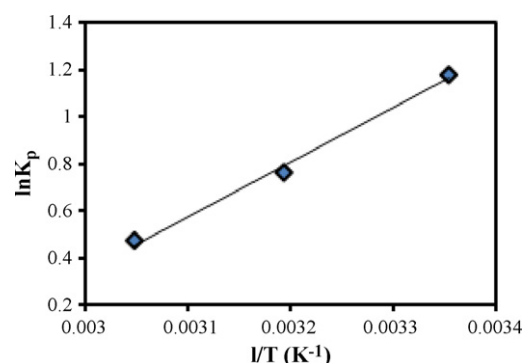
ΔG° (kJ mol ⁻¹)			ΔH° (kJ mol ⁻¹)	ΔS° (kJ mol ⁻¹ K ⁻¹)
298.15	313.15	328.15		
-2.93	-1.99	-1.29	-19.26	-0.0546

Table 5FTIR absorption frequencies (cm⁻¹) of CMCD-MNPs before and after adsorption and their possible assignments.

CMCD-MNPs (before adsorption)	CMCD-MNPs (after adsorption)	Assignment
582	586	νFe–O
947	946	Skeletal vibration involving α-1,4 linkage
1030	1028	ν _{as} C–O–C α-glycoside bridge
1080	1080	νC–C
1155	1153	νC–OH
–	1385	NO ₃ ⁻
1635	1628	νC=O (COO ⁻)
2924	2924	ν _{as} C–H
3423	3406	νO–H

ν: Stretching vibration; ν_{as}: asymmetric stretching vibration.

of metal ion adsorption onto magnetic nano-adsorbents. Moreover, the magnitude of ΔG° decreases with increasing temperature indicating that adsorption is not favorable at higher temperatures. The changes of enthalpy (ΔH°) and entropy (ΔS°) at 25–55 °C could be determined to be -19.26 kJ mol⁻¹ and -0.0546 kJ mol⁻¹ K⁻¹, respectively for CMCD-MNPs. The negative value of ΔH° confirms the exothermic nature of adsorption which is also supported by the decrease in value of Cu²⁺ uptake of the adsorbent with the rise in temperature. Similar results have been obtained for Cu²⁺ adsorption by cellulosic fibers modified by β-CD [49]. The negative entropy change (ΔS°) for the process is caused by the decrease in degree of freedom by the adsorbed species and indicates the stability of adsorption process with no structural change at solid-liquid interface [42,50].

**Fig. 10.** van't Hoff plot for the adsorption of Cu²⁺ by CMCD-MNPs.

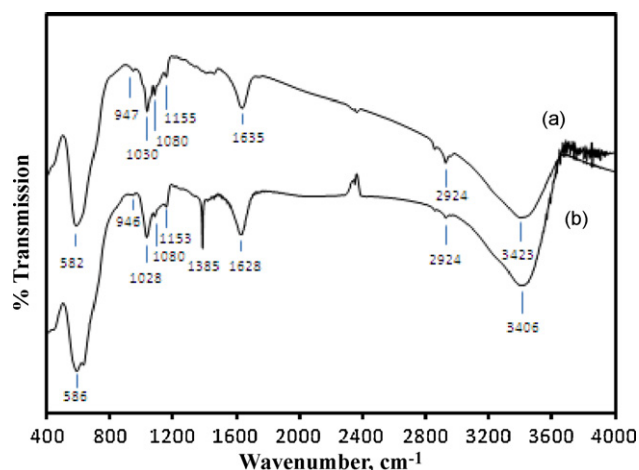


Fig. 11. FTIR spectra of CMCD-MNPs before (a) and after (b) adsorption of Cu²⁺.

3.2.5. Adsorption mechanisms

For understanding of the copper/CMCD-MNPs interaction, FTIR data are introduced to gain insight into the adsorption mechanism. Fig. 11 shows the spectra of CMCD-MNPs nano-adsorbent before and after Cu²⁺ adsorption and the possible IR frequencies of CMCD-MNPs are listed in Table 5. FTIR spectrum of metal (Cu²⁺)-sorbed CMCD-MNPs shows that the peaks expected at 1030, 1155, 1635 and 3423 cm⁻¹ have shifted, respectively to 1028, 1153, 1628 and 3406 cm⁻¹. The shifting of the peaks indicates that their corresponding functional groups (mainly hydroxyl and carbonyl groups) may directly be involved in interaction with metal to form surface complexes. Since Cu adsorption on the magnetic nano-adsorbent affected all the chemical bonds with oxygen atoms, it is reasonable to assume that the oxygen atoms would be the main adsorption sites for Cu attachment. After Cu²⁺ adsorption, a new sharp adsorption band at 1385 cm⁻¹ can also be observed which is assigned to nitrate (NO₃⁻) anion [51,52]. Hence, NO₃⁻ ions are on the surface of CMCD-MNPs to balance the electrical charges of the adsorbed copper ions [52]. In addition, the peak of Fe–O has a slight shift from 582 to 586 cm⁻¹ as some of metal ions are adsorbed onto the iron oxide [53].

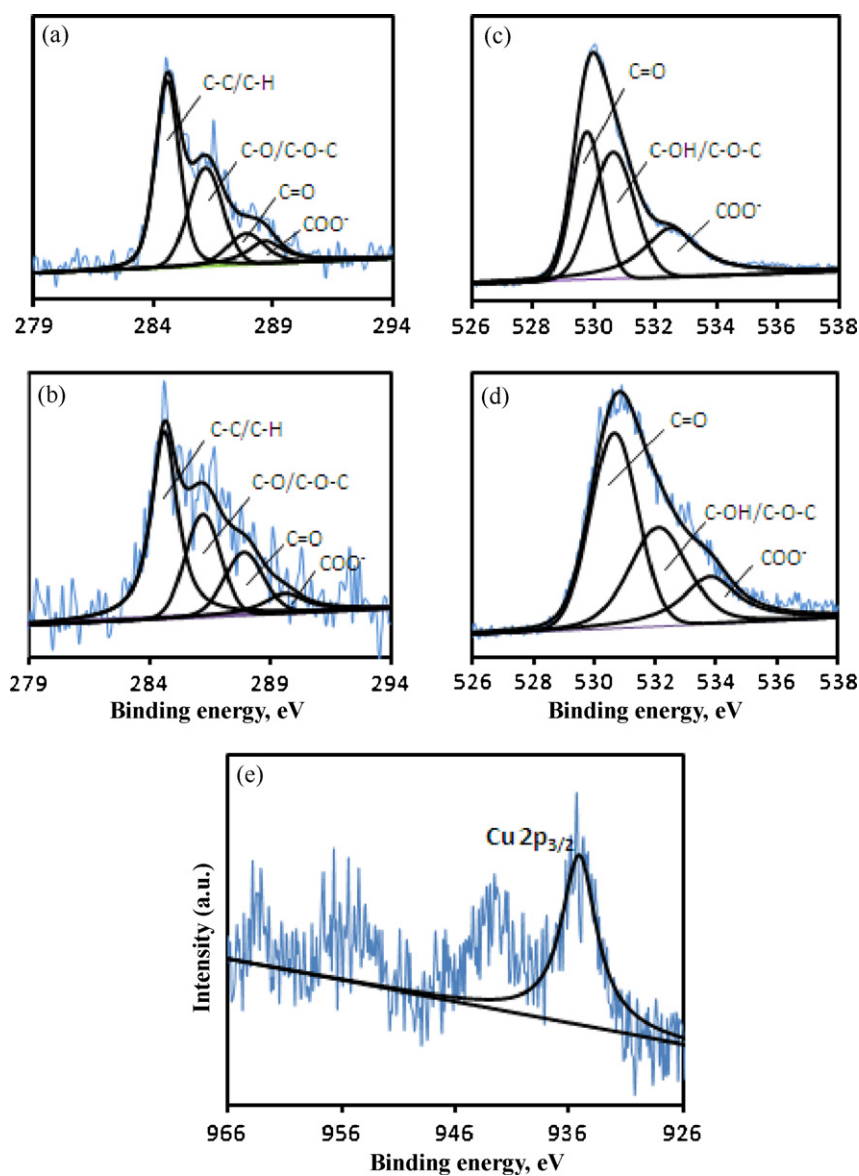


Fig. 12. XPS spectra of CMCD-MNPs: (a) C 1s before adsorption; (b) C 1s after adsorption; (c) O 1s before adsorption; (d) O 1s after adsorption; and (e) Cu(2p_{3/2}) core-level spectrum of Cu-loaded CMCD-MNPs.

To further verify the findings from the FTIR results, XPS studies of the CMCD-MNPs before and after Cu^{2+} adsorption are conducted. Fig. 12 shows the high resolution spectra of the C 1s and O 1s regions. Deconvolution of the C 1s peak produces four peaks of binding energies 284.6, 286.2, 287.9 and 288.7 eV, respectively (before and after Cu^{2+} adsorption) (Fig. 12a and b). These peaks can be assigned to the carbon atoms in the forms of C–C (aromatic), C–O (alcoholic hydroxyl and ether), C=O (carbonyl) and COO^- (carboxyl and ester) [31]. However, C 1s XPS spectra do not clearly show any significant changes of the CMCD-MNPs before and after Cu^{2+} adsorption which indicates that C atoms are not involved in chemical adsorption of Cu^{2+} .

Deconvolution of the O 1s peak yields three individual component peaks which come from different groups and overlap on each other (Fig. 12c and d). Peaks at 529.8 and 530.6 eV (before and after Cu^{2+} adsorption) are attributable to the C=O functional groups [31]. Peaks at 530.7 and 532.5 eV (observed before Cu^{2+} adsorption) and at 532.0 and 533.7 eV (observed after Cu^{2+} adsorption) are attributable to the C–O groups (alcoholic hydroxyl and ether) and COO^- groups, respectively. The shift in the binding energies after Cu^{2+} adsorption is likely to be caused by the binding of copper ions onto the oxygen atoms and thus reduces its electron density. Similar observation has been reported by Lim et al. [53] and Zheng et al. [31]. The relative content of oxygen in C–O (alcoholic hydroxyl and ether) is reduced (from 39.2% to 33.3%) and that in form of C=O increases (from 32.7% to 46.5%) after copper adsorption. These changes, together with binding energy shift, suggest that oxygen atoms are the main adsorption sites and the Cu^{2+} –O coordinate bonds are formed in Cu^{2+} adsorption by CMCD-MNPs, which is in good agreement with FTIR results.

Fig. 12e shows the $\text{Cu}(2p_{3/2})$ core-level spectrum of the CMCD-MNPs with adsorbed copper ions at pH 6.0. The binding energy of the copper at 935.1 eV and the presence of a satellite band nearby is representative of the oxidation state (+2) of copper for the $\text{Cu}(2p_{3/2})$ orbital [54,55]. This indicates the existence of Cu (i.e., Cu^{2+}) being adsorbed on the surface of the magnetic nano-adsorbents.

3.2.6. Desorption and regeneration studies

From practical point of view, repeated availability is a crucial factor for an advanced adsorbent [11,43,56]. Such adsorbent has higher adsorption capability as well as better desorption property which will reduce the overall cost for the adsorbent. To evaluate the possibility of regeneration and reusability of CMCD-MNPs as an adsorbent, we performed the desorption experiments. Desorption of Cu^{2+} from CMCD-MNPs was demonstrated using three different eluent buffers, namely 0.1 M citric acid, 0.1 M Na_2EDTA and 0.1 M acetic acid. It is found that the quantitative desorption efficiencies using citric acid, Na_2EDTA and acetic acid were 96.2, 89.4 and 66.8%, respectively. The reusability was checked by following the adsorption–desorption process for three cycles and the adsorption efficiency in each cycle was analyzed. In each cycle, 120 mg of CMCD-MNPs and 10 mL of an initial Cu^{2+} concentration of 200 mg/L was used for the adsorption process, and 10 mL of 0.1 M citric acid was used as desorption eluent. The desorption kinetics of Cu^{2+} from Cu-loaded nanoparticles and the adsorption and desorption capacity of CMCD-MNPs is presented in Fig. 13. It is observed that the desorption reaches equilibrium within 1 h using 0.1 M citric acid solution as desorption eluent. Cu^{2+} adsorption capacity of CMCD-MNPs remains almost constant for the three cycles, indicating that there are no irreversible sites on the surface of CMCD-MNPs. Recently Hu et al. [12] reported that β -cyclodextrin grafted MWCNTs/iron oxides/CD can be recycled five times for Pb(II) adsorption with less than 5% of decline in efficiency, indicating good reusability of the adsorbents. Our recyclability studies suggest that these nano-adsorbents can be repeatedly used as efficient adsorbents in wastewater treatment.

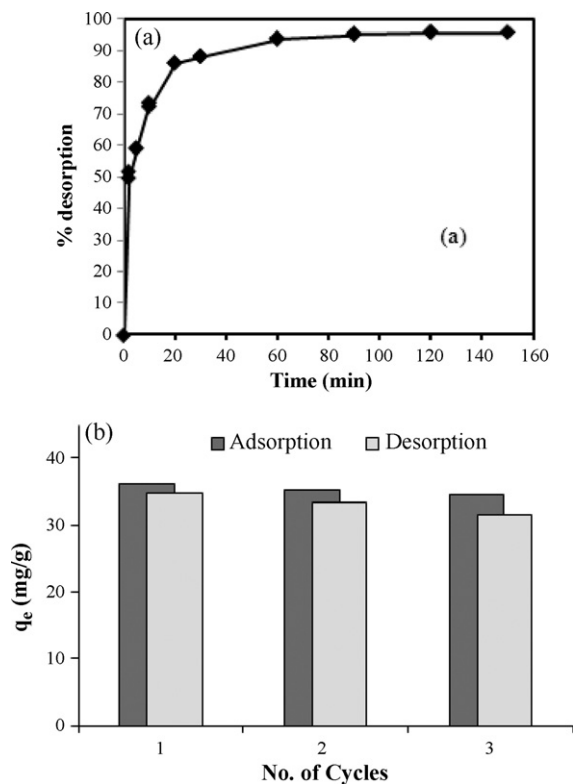


Fig. 13. (a) Kinetics of desorption of Cu^{2+} from Cu-loaded CMCD-MNPs in 0.1 M citric acid solution; (b) performance of CMCD-MNPs by multiple cycles of regeneration.

4. Conclusions

In this study, we have successfully synthesized a magnetic novel nano-adsorbent comprising Fe_3O_4 nanoparticles modified with CM- β -CD having magnetic properties exhibited by magnetite and adsorption properties of CM- β -CD. Grafting of CM- β -CD onto the magnetic nano-adsorbents is confirmed by FTIR, TGA, and XPS analyses. These magnetic nano-adsorbents can effectively be used to remove Cu^{2+} from aqueous solution. The solution pH greatly affects the adsorption of Cu^{2+} onto CMCD-MNPs. Adsorption of Cu^{2+} reaches equilibrium within 30 min and 90% of Cu^{2+} is being adsorbed at 15 min. The kinetics of Cu^{2+} adsorption follows the pseudo-second-order model. The equilibrium data are fitted well by the Langmuir model of adsorption. The maximum adsorption capacity of CMCD-MNPs, determined to be 47.2 mg/g, is considerably higher than that of some other reported magnetic adsorbents. Both FTIR and XPS analyses clearly reveal that the oxygen atoms on CMCD-MNPs are the main binding sites for Cu^{2+} to form surface-complexes. In addition, the copper ions can be desorbed effectively from CMCD-MNPs by treatment with citric acid and Na_2EDTA solution. Results of this work suggest that the CMCD-MNPs may be promising adsorbents for the removal of heavy metal ions from wastewater using the technology of magnetic separation.

References

- O. Ozay, S. Ekici, Y. Baran, N. Aktas, N. Sahiner, Removal of toxic metal ions with magnetic hydrogels, *Water Res.* 43 (2009) 4403–4411.
- Y.T. Zhou, H.L. Nie, C. Branford-White, Z.Y. He, L.M. Zhu, Removal of Cu^{2+} from aqueous solution by chitosan-coated magnetic nanoparticles modified with α -ketoglutaric acid, *J. Colloid Interface Sci.* 330 (2009) 29–37.
- R.W. Rousseau (Ed.), *Handbook of Separation Process Technology*, Wiley, New York, 1987.
- H. Chen, Y. Zhao, A. Wang, Removal of Cu(II) from aqueous solution by adsorption onto acid-activated palygorskite, *J. Hazard. Mater.* 149 (2007) 346–354.
- S.S. Banerjee, D.H. Chen, Fast removal of copper ions by gum arabic modified magnetic nano-adsorbent, *J. Hazard. Mater.* 147 (2007) 792–799.

- [6] S.F. Lim, Y.M. Zheng, S.W. Zou, J.P. Chen, Removal of copper by calcium alginate encapsulated magnetic sorbent, *Chem. Eng. J.* 152 (2009) 509–513.
- [7] Y.C. Chang, D.H. Chen, Preparation and adsorption properties of monodisperse chitosan-bound Fe₃O₄ magnetic nanoparticles for removal of Cu(II) ions, *J. Colloid Interface Sci.* 283 (2005) 446–451.
- [8] S.H. Huang, D.H. Chen, Rapid removal of heavy metal cations and anions from aqueous solutions by an amino-functionalized magnetic nano-adsorbent, *J. Hazard. Mater.* 163 (2009) 174–179.
- [9] Ç. Üzümlü, T. Shahwan, A. Eroğlu, K. Hallam, T. Scott, I. Lieberwirth, Synthesis and characterization of kaolinite-supported zero-valent iron nanoparticles and their application for the removal of aqueous Cu²⁺ and Co²⁺ ions, *Appl. Clay Sci.* 43 (2009) 172–181.
- [10] C.L. Chen, X.K. Wang, M. Nagatsu, Europium adsorption on multiwall carbon nanotube/iron oxide magnetic composite in the presence of polyacrylic acid, *Environ. Sci. Technol.* 43 (2009) 2362–2367.
- [11] C. Chen, J. Hu, D. Shao, J. Li, X. Wang, Adsorption behavior of multiwall carbon nanotube/iron oxide magnetic composites for Ni(II) and Sr(II), *J. Hazard. Mater.* 164 (2009) 923–928.
- [12] J. Hu, D. Shao, C. Chen, G. Sheng, J. Li, X. Wang, M. Nagatsu, Plasma-induced grafting of cyclodextrin onto multiwall carbon nanotube/iron oxides for adsorbent application, *J. Phys. Chem. B* 114 (2010) 6779–6785.
- [13] L.C.A. Oliveira, D.I. Petkowicz, A. Smianotto, S.B.C. Pergher, Magnetic zeolites: a new adsorbent for removal of metallic contaminants from water, *Water Res.* 38 (2004) 3699–3704.
- [14] L.C.A. Oliveira, R.V.R.A. Rios, J.D. Fabris, V. Garg, K. Sapag, R.M. Lago, Activated/carbon iron oxide magnetic composites for the adsorption of contaminants in water, *Carbon* 40 (2002) 2177–2183.
- [15] J.F. Liu, Z.S. Zhao, G.B. Jiang, Coating Fe₃O₄ magnetic nanoparticles with humic acid for high efficient removal of heavy metals in water, *Environ. Sci. Technol.* 42 (2008) 6949–6954.
- [16] M. Ozmen, K. Can, G. Arslan, A. Tor, Y. Cengeloglu, M. Ersoz, Adsorption of Cu(II) from aqueous solution by using modified Fe₃O₄ magnetic nanoparticles, *Desalination* 254 (2010) 162–169.
- [17] Y.T. Zhou, C. Branford-White, H.L. Nie, L.M. Zhu, Adsorption mechanism of Cu²⁺ from aqueous solution by chitosan-coated magnetic nanoparticles modified with α-ketoglutaric acid, *Colloids Surf. B: Biointerfaces* 74 (2009) 244–252.
- [18] J. Szejtli, Introduction and general overview of cyclodextrin chemistry, *Chem. Rev.* 98 (1998) 1743–1754.
- [19] M.V. Rekharsky, Y. Inoue, Complexation thermodynamics of cyclodextrins, *Chem. Rev.* 98 (1998) 1875–1918.
- [20] E. Norkus, Metal ion complexes with native cyclodextrins: An overview, *J. Inclusion Phenom. Macrocyclic Chem.* 65 (2009) 237–248.
- [21] M.E. Skold, G.D. Thyne, J.W. Drexler, J.E. McCray, Solubility enhancement of seven metal contaminants using carboxymethyl-beta-cyclodextrin (CMCD), *J. Contam. Hydrol.* 107 (2009) 108–113.
- [22] X. Wang, M.L. Brusseau, Simultaneous complexation of organic compounds and heavy metals by a modified cyclodextrin, *Environ. Sci. Technol.* 29 (1995) 2632–2635.
- [23] M.L. Brusseau, X. Wang, W.J. Wang, Simultaneous elution of heavy metals and organic compounds from soil by cyclodextrin, *Environ. Sci. Technol.* 31 (1997) 1087–1092.
- [24] L.A. Belyakova, K.A. Kazdobin, V.N. Belyakov, S.V. Ryabov, A.F. Danil de Namor, Synthesis and properties of supramolecular systems based on silica, *J. Colloid Interface Sci.* 283 (2005) 488–494.
- [25] C.A. Kozłowski, T. Girek, W. Walkowiak, J. Kozłowska, The effect of β-CD polymers structure on the efficiency of copper(II) ion flotation, *J. Inclusion Phenom. Macrocyclic Chem.* 55 (2006) 71–77.
- [26] E. Furusaki, Y. Ueno, N. Sakairi, N. Nishi, S. Tokura, Facile preparation and inclusion ability of a chitosan derivative bearing carboxymethyl-β-cyclodextrin, *Carbohydr. Polym.* 29 (1996) 29–34.
- [27] A.Z.M. Badruddoza, K. Hidajat, M.S. Uddin, Synthesis and characterization of beta-cyclodextrin-conjugated magnetic nanoparticles and their uses as solid-phase artificial chaperones in refolding of carbonic anhydrase bovine, *J. Colloid Interface Sci.* 346 (2010) 337–346.
- [28] A. Badruddoza, G.S.S. Hazel, K. Hidajat, M. Uddin, Synthesis of carboxymethyl-β-cyclodextrin conjugated magnetic nano-adsorbent for removal of methylene blue, *Colloids Surf. A: Physicochem. Eng. Aspects* 367 (2010) 85–95.
- [29] B.J. Ravoo, R. Darcy, A. Mazzaglia, D. Nolan, K. Gaffney, Supramolecular tapes formed by a cationic cyclodextrin in water, *Chem. Commun.* 9 (2001) 827–828.
- [30] S.S. Banerjee, D.H. Chen, Cyclodextrin conjugated magnetic colloidal nanoparticles as a nanocarrier for targeted anticancer drug delivery, *Nanotechnology* 19 (2008) 265601–265607.
- [31] J.C. Zheng, H.M. Feng, M.H.W. Lam, P.K.S. Lam, Y.W. Ding, H.Q. Yu, Removal of Cu(II) in aqueous media by biosorption using water hyacinth roots as a biosorbent material, *J. Hazard. Mater.* 171 (2009) 780–785.
- [32] D. Caruntu, G. Caruntu, Y. Chen, C. O'Connor, G. Goloverda, V. Kolesnichenko, Synthesis of variable-sized nanocrystals of Fe₃O₄ with high surface reactivity, *Chem. Mater.* 16 (2004) 5527.
- [33] M.H. Liao, D.H. Chen, Preparation and characterization of a novel magnetic nano-adsorbent, *J. Mater. Chem.* 12 (2002) 3654–3659.
- [34] M.H. Kalavathy, L.R. Miranda, Comparison of copper adsorption from aqueous solution using modified and unmodified *Hevea brasiliensis* saw dust, *Desalination* 255 (2010) 165–174.
- [35] G. Sheng, J. Li, D. Shao, J. Hu, C. Chen, Y. Chen, X. Wang, Adsorption of copper(II) on multiwalled carbon nanotubes in the absence and presence of humic or fulvic acids, *J. Hazard. Mater.* 178 (2010) 333–340.
- [36] H. Chen, G. Dai, J. Zhao, A. Zhong, J. Wu, H. Yan, Removal of copper(II) ions by a biosorbent – *Cinnamomum camphora* leaves powder, *J. Hazard. Mater.* 177 (2010) 228–236.
- [37] G. Zhao, H. Zhang, Q. Fan, X. Ren, J. Li, Y. Chen, X. Wang, Sorption of copper(II) onto super-adsorbent of bentonite–polyacrylamide composites, *J. Hazard. Mater.* 173 (2010) 661–668.
- [38] S. Deng, R. Bai, J.P. Chen, Aminated polyacrylonitrile fibers for lead and copper removal, *Langmuir* 19 (2003) 5058–5064.
- [39] Y.S. Ho, G. McKay, A comparison of chemisorption kinetic models applied to pollutant removal on various sorbents, *Proc. Saf. Environ. Protect.* 76 (1998) 332–340.
- [40] Y. Ho, G. McKay, Pseudo-second order model for sorption processes, *Process Biochem.* 34 (1999) 451–465.
- [41] O. Yavuz, Y. Altunkaynak, F. Güzel, Removal of copper, nickel, cobalt and manganese from aqueous solution by kaolinite, *Water Res.* 37 (2003) 948–952.
- [42] A. Kamari, W.S.W. Ngah, Isotherm, kinetic and thermodynamic studies of lead and copper uptake by H₂SO₄ modified chitosan, *Colloids Surf. B: Biointerfaces* 73 (2009) 257–266.
- [43] C. Chen, X. Wang, Adsorption of Ni(II) from aqueous solution using oxidized multiwall carbon nanotubes, *Ind. Eng. Chem. Res.* 45 (2006) 9144–9149.
- [44] S. Yang, J. Li, D. Shao, J. Hu, X. Wang, Adsorption of Ni(II) on oxidized multiwalled carbon nanotubes: effect of contact time, pH, foreign ions and PAA, *J. Hazard. Mater.* 166 (2009) 109–116.
- [45] J. Wang, S. Zheng, Y. Shao, J. Liu, Z. Xu, D. Zhu, Amino-functionalized Fe₃O₄@SiO₂ core-shell magnetic nanomaterial as a novel adsorbent for aqueous heavy metals removal, *J. Colloid Interface Sci.* 349 (2010) 293–299.
- [46] M. Bystrzyjewski, K. Pyrzyńska, A. Huczko, H. Lange, Carbon-encapsulated magnetic nanoparticles as separable and mobile sorbents of heavy metal ions from aqueous solutions, *Carbon* 24 (1994) 19–44.
- [47] J. Wu, H.Q. Yu, Biosorption of 2,4-dichlorophenol from aqueous solution by *Phanerochaete chrysosporium* biomass: isotherms, kinetics and thermodynamics, *J. Hazard. Mater.* 137 (2006) 498–508.
- [48] G.Z. Kyzas, M. Kostoglou, N.K. Lazaridis, Copper and chromium(VI) removal by chitosan derivatives—Equilibrium and kinetic studies, *Chem. Eng. J.* 152 (2009) 440–448.
- [49] Y. Xia, J. Wan, Preparation and adsorption of novel cellulosic fibers modified by -cyclodextrin, *Polym. Adv. Technol.* 19 (2008) 270–275.
- [50] T. Aman, A.A. Kazi, M.U. Sabri, Q. Bano, Potato peels as solid waste for the removal of heavy metal copper(II) from waste water/industrial effluent, *Colloids Surf. B: Biointerfaces* 63 (2008) 116–121.
- [51] W. West, *Chemical Applications of Spectroscopy*, Interscience, New York, 1956.
- [52] C. Liu, R. Bai, Q. San Ly, Selective removal of copper and lead ions by diethylenetriamine-functionalized adsorbent: behaviors and mechanisms, *Water Res.* 42 (2008) 1511–1522.
- [53] S.F. Lim, Y.M. Zheng, S.W. Zou, J.P. Chen, Characterization of copper adsorption onto an alginate encapsulated magnetic sorbent by a combined FT-IR, XPS, and mathematical modeling study, *Environ. Sci. Technol.* 42 (2008) 2551–2556.
- [54] N. Li, R. Bai, Copper adsorption on chitosan–cellulose hydrogel beads: behaviors and mechanisms, *Sep. Purif. Technol.* 42 (2005) 237–247.
- [55] J. Kang, H. Liu, Y.M. Zheng, J. Qu, J.P. Chen, Systematic study of synergistic and antagonistic effects on adsorption of tetracycline and copper onto a chitosan, *J. Colloid Interface Sci.* 344 (2010) 117–125.
- [56] G. Sheng, S. Wang, J. Hu, Y. Lu, J. Li, Y. Dong, X. Wang, Adsorption of Pb(II) on diatomite as affected via aqueous solution chemistry and temperature, *Colloids Surf. A: Physicochem. Eng. Aspects* 339 (2009) 159–166.